Mechanistic Insight Provided by Glutaredoxin within a Fusion to Redox-Sensitive Yellow Fluorescent Protein

Olof Björnberg,[‡] Henrik Østergaard,[§] and Jakob R. Winther*,[||]

Carlsberg Laboratory, DK-2500 Copenhagen Valby, Denmark

Received November 3, 2005; Revised Manuscript Received December 21, 2005

ABSTRACT: Redox-sensitive yellow fluorescent protein (rxYFP) contains a dithiol disulfide pair that is thermodynamically suitable for monitoring intracellular glutathione redox potential. Glutaredoxin 1 (Grx1p) from yeast is known to catalyze the redox equilibrium between rxYFP and glutathione, and here, we have generated a fusion of the two proteins, rxYFP−Grx1p. In comparison to isolated subunits, intramolecular transfer of reducing equivalents made the fusion protein kinetically superior in reactions with glutathione. The rate of GSSG oxidation was thus improved by a factor of 3300. The reaction with GSSG most likely takes place entirely through a glutathionylated intermediate and not through transfer of an intramolecular disulfide bond. However, during oxidation by H_2O_2, hydroxyethyl disulfide, or cystine, the glutaredoxin domain reacted first, followed by a rate-limiting (0.13 min^{-1}) transfer of a disulfide bond to the other domain. Thus, reactivity toward other oxidants remains low, giving almost absolute glutathione specificity. We have further studied CPYC → CPYS variants in the active site of Grx1p and found that the single Cys variant had elevated oxidoreductase activity separately and in the fusion. This could not be ascribed to the lack of an unproductive side reaction to glutaredoxin disulfide. Instead, slower alkylation kinetics with iodoacetamide indicates a better leaving-group capability of the remaining cysteine residue, which can explain the increased activity.

Green fluorescent protein (GFP)[1] has gained tremendous interest as a noninvasive marker in cell biology for investigations of, e.g., protein localization. It is a stable single-chain protein (M_r = 27 kDa) whose fluorescence properties arise from a centrally buried chromophore formed by a self-catalyzed intramolecular cyclization of three residues (Ser65−Tyr66−Gly67) (reviewed in ref *1*). To extend the applicability of GFP, it has been modified through direct manipulation or fusion to other proteins. Recently, cysteine residues capable of forming disulfides were introduced close to the chromophore to obtain redox sensors. A derivative of GFP, YFP (yellow fluorescent protein) was used as a template by Ostergaard et al. (*2*) to construct redox-sensitive YFP (rxYFP), containing a cysteine pair at positions 149 and 202. Formation of a disulfide bond between these residues, situated on adjacent β strands, results in a strong quenching of fluorescence. Employing GFP as a template, Hanson et al. (*3*) created redox-sensitive GFPs (roGFPs), where the cysteine residues were introduced at positions 147−204 (roGFP 1 and 2) and 149−202 (roGFP 3 and 4, the equivalent positions of rxYFP). The roGFPs have the advantage over rxYFP of exhibiting ratiometric spectral shifts. rxYFP and roGFP have been used to monitor the redox status in the yeast *Saccharomyces cerevisiae* and mammalian cells, respectively (*3*−*5*).

Similar to other proteins, the redox sensor leaves the ribosome in the reduced state and must subsequently interact with cellular redox conditions to attain a steady-state level of oxidation. Because thiol−disulfide redox reactions can be slow at neutral pH in the absence of catalyzing enzymes, the identification of relevant catalysts for the reaction is crucial for determining what redox couple is measured *in vivo*. For rxYFP, it was found that the steady state was reached very slowly in yeast deficient in glutaredoxins and that yeast glutaredoxin 1 (Grx1p), *in vitro*, efficiently equilibrated the sensor with a glutathione redox buffer. Furthermore, no thiol disulfide exchange was detected with the protein disulfide reductant thioredoxin, and on the basis of these observations, it was concluded that determination of the redox potential of the cytosolic glutathione redox pair using rxYFP depends upon the presence of glutaredoxin (Grx) (*4*).

Grx's, also referred to as thioltransferases, are small (ca 10 kDa) heat-stable redox proteins belonging to the same superfamily as thioredoxins, with an active-site sequence motif CXXC (*6*, *7*). Although there are cases of functional overlap between thioredoxin and Grx as protein disulfide

* To whom correspondence should be addressed. Institute of Molecular Biology and Physiology, Department of Biochemistry, Universitetsparken 13, 2100 Copenhagen, Denmark. Telephone: +45-3532-1500. Fax: +45-3532-1567. E-mail: jrwinther@aki.ku.dk.

[‡] Present address: Department of Cell and Organism Biology, Lund University, SE-22362, Lund, Sweden.

[§] Present address: Novo Nordisk A/S, DK-2760 Måløv, Denmark.

[||] Present address: Department of Biochemistry, Institute of Molecular Biology and Physiology, August Krogh Building, DK-2100 Copenhagen, Denmark.

[1] Abbreviations: GFP, green fluorescent protein; Grx, glutaredoxin; Grx1p, glutaredoxin 1 of yeast; Grx1p-sC, mutant Grx1p with the active-site sequence CPYS; Grx(SSG)(SH), Grx in the mixed disulfide intermediate; GSH, glutathione; GSSG, glutathione disulfide; HED, β-hydroxyethyl disulfide; rxYFP, redox-sensitive yellow fluorescent protein; rxYFP−Grx1p, fusion protein of rxYFP and Grx1p; rxYFP−Grx1p-sC, fusion protein of rxYFP and Grx1p-sC.

10.1021/bi0522495 CCC: $33.50
Published on Web 01/31/2006

Scheme 1: Two Half Reactions in the Glutaredoxin Assay

Half reaction 1:

$$RSSG + Grx(SH)_2 \Rightarrow RSH + Grx(SSG)(SH)$$

Half reaction 2:

$$GSH + Grx(SSG)(SH) \Rightarrow GSSG + Grx(SH)_2$$

Possible side reaction:

$$Grx(SSG)(SH) \Rightarrow Grx\text{-}S_2 + GSH$$

reductants, e.g., as the hydrogen donor for ribonucleotide reductase, the two protein families differ with respect to the substrate specificity and reduction system. Grx is reduced by glutathione (GSH), whereas thioredoxin is reduced by thioredoxin reductase. Both systems ultimately rely on NADPH as an electron donor (*6*). In addition to a dithiol pathway for the reduction of a disulfide, Grx follows a monothiol pathway in the reduction of a mixed disulfide with glutathione, as evidenced by the ability of mutant monothiol Grx (CXXS) to carry out the reaction (*8*). Furthermore, kinetic evidence for a preferred monothiol pathway (half reactions 1 and 2 in Scheme 1) was presented by Gravina and Mieyal (*9*). The three dithiol Grx's from *Escherichia coli* (reviewed in ref *7*) are particularly well-understood; their levels of expression have been analyzed in detail, and their structures have been resolved by NMR. The monothiol Grx4 was recently characterized (*10*, *11*). *S. cerevisiae* contains five Grx's. The cytosolic Grx1p and Grx2p, both involved in the response to oxidative stress (*12*), belong to the typical dithiol form (CPYC), while the other three are, like *E. coli* Grx4, monothiol Grx's with the active-site sequence CGFS. Grx3p and Grx4p are localized in the nucleus, and Grx5p participates in the assembly of iron−sulphur clusters in mitochondria (*13*). Two dithiol Grx's have been isolated from human cells, the predominant Grx1 with mainly cytoplasmic location and Grx2 with both nuclear and mitochondrial isoforms (*14*−*16*). Human Grx1 has been suggested to be involved in both signal transduction and radical scavenging (*17*, *18*).

We were interested in characterizing the interaction between yeast Grx1p and its synthetic substrate rxYFP and obtaining a redox sensor independent of the availability of Grx in the experimental host organism. We therefore constructed a fusion of the two proteins, rxYFP−Grx1p, which efficiently equilibrates the sensor with a glutathione redox buffer and provides new insight into the mechanism of Grx.

EXPERIMENTAL PROCEDURES

Materials. Enzymes for the modification of DNA were from New England BioLabs, and oligonucleotides were obtained from MWG-Biotech (Germany). Analytical chemicals [DTT, NADPH, GSH, GSSG, hydroxyethyl disulfide (HED), cystine, glutathione reductase, and cystamine dihydrochloride] were purchased from Sigma, Fluka, or Merck. PD10 and NAP5 columns and Q-sepharose were from Amersham Bioscience. The His-bind resin was from Novagen. The reactive polymer mPEG−maleimide (5000 Da) was from Nektar. NuPAGE Novex Bis-Tris Gels (12%) were bought from Invitrogen.

Construction of the Fusion Protein rxYFP−Grx1p. The coding regions of rxYFP and Grx1p were fused by overlap extension in PCR (*19*) using four primers. As templates, we used the plasmid pHOJ124, containing the reading frame of rxYFP as described (*2*), and genomic yeast DNA (*S. cerevisiae*, strain S288C) for the Grx1p gene. The primer 5rxYFP (TAGGAGGC*CATATG*TCTAAAGGTGAAGAACTG) contained an *Nde*I site at the start of the rxYFP reading frame and was used in the first PCR together with 3rxYFP (CATGCCGGAACCAGAGCCGGAACCAGATTTATACAGCTCATGCATGCCATGCGT), which replaced the stop codon of rxYFP by a serine codon followed by seven alternating glycine and serine codons. In the second PCR, the Grx1p gene was amplified by the primers 5Grx-1 (AAATCTGGTTCCGGCTCTGGTTCCGGCATGGTATCTCAAGAAACTATCAA GCACGTC) and 3Grx-1 (GTCAGCT*CTCGAG*ATTTGCAAGAATAGGTTCTAACAATTCCTC). Primer 5Grx-1 harbored the complementary changes of 3rxYFP and the first 10 codons of Grx1p, and primer 3Grx-1 removed the stop codon of the Grx1p gene and introduced an *Xho*I site (in italics). The two PCR products obtained, covering the two genes, were purified on Qiaquick columns (Qiagen) and used in a third PCR with 5rxYFP and 3Grx-1 as flanking primers. The final PCR product containing the fused genes was inserted into the pCR-XL-TOPO plasmid (Invitrogen), and using the *Nde*I and *Xho*I sites, the insert was moved to the pET-24a(+) plasmid (Novagen). The cloning in the *Xho*I site results in two additional residues, leucine and glutamate, followed by a hexahistidine "tag" at the C terminus of the translated protein. The insert of the new plasmid (pOB1) was verified by sequencing.

Construction of rxYFP−Grx1p-sC and Grx1p-sC. Plasmid pOB1, encoding rxYFP−Grx1p, was used as a template for mutagenesis according to the "QuickChange procedure" as described by Stratagene. The two mutant primers, Cys276S5 (ACGTACTGTCCATACTCTCATGCAGC*TTTAAA*CACGCTTTTTGAAAAG) and Cys276S3 (G*TTTAAA*GCTGCATGAGAGTATGGACAGTACGTTTTGGA) were designed to change the cysteine codon (TGT) of the second cysteine (C276) in the Grx domain to a serine codon (TCT). Furthermore, to facilitate the subsequent screening, the primers introduced a *Dra*I restriction site (in italics), which was silent with respect to the translation product. In a separate construct, the same mutant primers were used to change the second cysteine (C30) of Grx1p into serine. As a template, we used pHOJ167, a pET-24a(+)-based plasmid encoding Grx1p (*4*). The rxYFP−Grx1p-sC and Grx1p-sC reading frames in the plasmids, called pOB2 and pOB3, were confirmed by sequencing.

Expression and Purification of Proteins. The fusion proteins, rxYFP−Grx1p and rxYFP−Grx1p-sC, as well as Grx1p and Grx1p-sC, were expressed in the strain BL21-(DE3) (Novagen) essentially as described for rxYFP (*2*). Extraction was performed by 10 freeze/thaw cycles in 10 mM imidazole, 50 mM potassium phosphate, and 0.3 M NaCl at pH 7.8 (binding buffer) and followed by centrifugation at 17000*g* for 45 min. The cleared extract was loaded onto a column (1.6 × 4 cm) with His-bind resin (Novagen) and washed with 5 volumes of binding buffer and 5 volumes of 20 mM imidazole, 50 mM potassium phosphate, and 0.3 M NaCl at pH 7.8. Proteins were eluted with 0.25 M

imidazole, 50 mM potassium phosphate, and 0.3 M NaCl at pH 7.8. The final yield of fusion protein from 0.5 L of bacteria was typically 20 mg. Expression and purification of Grx1p and its mutant form Grx1p-sC followed the same steps until the His-bind resin. The eluted protein was dialyzed against 20 mM potassium phosphate and 1 mM EDTA at pH 7.5, applied onto a Q-Sepharose column (1.6 × 4 cm) previously equilibrated in dialysis buffer, and eluted again by a gradient of NaCl (0−0.5 M) in dialysis buffer. To avoid the formation of dimers (*8*), 1 mM DTT was included during dialysis and Q-Sepharose chromatography of Grx1p-sC. Final yields of Grx1p and Grx1p-sC were ca. 40 mg/0.5 L of bacteria.

Protein and Reagent Quantifications. Absorption was measured on a Perkin−Elmer UV/vis 16 spectrometer. The concentration of rxYFP and its two fusion variants was determined by denaturation (0.1 M NaOH) and absorbance measurement at 447 nm of the base-denatured chromophore using an extinction coefficient of 44 000 M^{-1} cm^{-1} (*20*). Concentrations of Grx1p and Grx1p-sC were assessed using a theoretical protein extinction coefficient of 5200 M^{-1} cm^{-1} at 280 nm (*21*). The difference between the dithiol, monothiol, or disulfide form (<200 M^{-1} cm^{-1}) was considered negligible. The thiol content of reduced and desalted protein and of stock solutions of GSH and DTT was determined with Ellman's reagent (13 600 M^{-1} cm^{-1} at 412 nm) (*22*). Stock solutions of GSSG were quantified by absorption at 248 nm [382 M^{-1} cm^{-1} (*23*)].

Glutaredoxin Assay. The glutaredoxin assay, also referred to as the GSH−disulfide transhydrogenase (oxidoreductase) or thioltransferase assay, involves a coupled system where the GSSG generated (half reaction 2 in Scheme 1) is reduced by glutathione reductase and NADPH. The assay was carried out according to Holmgren and Åslund (*24*) in 0.1 M Tris-HCl at pH 8.0, 2 mM EDTA, 0.1 mg/mL bovine serum albumin, 1 mM GSH, 0.7 mM HED, and 6 μg/mL glutathione reductase at 25 °C. However, the NADPH concentration was reduced from 0.4 to 0.3 mM, and 1.0 mL cuvettes were used.

Redox Reaction Conditions. Generally, a standard buffer consisting of 100 mM potassium phosphate and 1 mM EDTA at pH 7.0 saturated with argon was used at 30 °C. The exceptions were the alkylation reactions at 0 °C in standard buffer (also saturated with argon) and the glutaredoxin assay (25 °C and pH 8.0).

Fluorimetric Measurements. The fluoresence measurements were performed in a Perkin−Elmer luminiscence spectrometer LS50B with a thermostated (30 °C) stirred single-cell holder. The excitation and emission wavelengths were 512 and 523 nm, respectively, using slit widths between 2 and 3.5 nm. The reaction volume was usually 2 mL in a 3 mL 1 × 1 cm quartz cuvette from Hellma. The concentration of the redox sensor was 0.3 ± 0.1 μM, and oxidants or reductants were added by pipetting. The reduced forms of the redox sensors were obtained by reduction with DTT for 1 h at pH 8.0 at room temperature, followed by gel-filtration on PD10 or NAP5 columns previously equilibrated in standard buffer saturated with argon.

Determination of Redox Potential. The equilibrium constant, K_{ox}, in standard buffer (pH 7.0) for the reaction: rxYFP−$Grx1p_{red}$ + GSSG ⇔ rxYFP−$Grx1p_{ox}$ + 2 GSH, was determined by fluorescence according to Ostergaard et al. (*4*). However, no additional Grx was required because the fusion protein catalyzed its own equilibration with the glutathione buffer. The concentration of GSSG at equilibrium was determined on acid-quenched samples by HPLC (*4*). K_{ox} was converted to standard redox potential (E_0') by the Nernst equation using a value of −240 mV for the GSH/GSSG redox couple (*25*).

Protection of Reduced Grx1p from Modification with mPEG−Maleimide. Reduced and desalted Grx1p (50 μM) was incubated during 15 min on an ice bath in standard buffer with the oxidants H_2O_2, HED, cystine, and cystamine (0.5 mM) before the addition of mPEG−maleimide (0.6 mM). Protein modification was assessed by retarded migration on 12% reducing SDS−PAGE gels.

Alkylation of Grx1p and Grx1p-sC. Reduced and desalted Grx1p and Grx1p-sC had a thiol content per enzyme molecule of 1.8−2.0 and 0.9−1.0, respectively. Alkylations were performed on ice (0 °C), and preliminary experiments were set up to find suitable pseudo-first-order conditions. The reaction was started by adding ice-cold iodoacetamide (200 μM). Samples were taken at intervals and quenched by a 10-fold dilution in standard buffer supplemented with 0.1 mM GSSG and 0.1 mg/mL bovine serum albumin. A sample representing 0 min was taken before the reaction, and the time samples were assayed in the glutaredoxin assay (*24*).

Data Analysis. Monophasic first-order reaction traces from oxidation and reduction of redox sensors as well as the disappearance of activity during alkylation were evaluated using the software Kaleidagraph (Synergy Software). A biphasic fit was used for oxidations of rxYFP−Grx1p and rxYFP−Grx1p-sC by GSSG. The figures were also generated using Kaleidagraph.

RESULTS

Construction of the Fusion Protein. We constructed a fusion protein consisting of an enzyme (Grx1p), which was to act intramolecularly on a covalently linked substrate (rxYFP). It was considered crucial to incorporate sufficient distance and flexibility between the domains and at the same time minimize the risk of proteolysis.

The last 7 C-terminal residues of rxYFP were not defined in its X-ray structure (*2*), and these residues can be deleted in GFP without affecting fluorescence properties (*26*). The C terminus of rxYFP furthermore extends from a β strand on the same face of the protein as the cysteine pair. We therefore chose rxYFP as the N-terminal partner in the fusion, rxYFP−Grx1p. To improve mutual flexibility, the rxYFP domain was connected to the Grx domain by a linker of 8 residues, consisting of alternating serine and glycine residues $(Ser−Gly)_4$. Expression of rxYFP−Grx1p in yeast cells indicated that the linker was resistant to proteases because only the full-length protein was detected by Western blots (data not shown). Recombinant protein from *E. coli* was obtained in reasonable yield, and the two domains of rxYFP−Grx1p were only slightly affected in their intrinsic properties. Excitation and emission spectra were close to identical with those of rxYFP. However, upon reduction by DTT, the increase in emission intensity (at 523 nm) was slightly lower (2.1-fold, as compared to 2.2-fold for rxYFP).

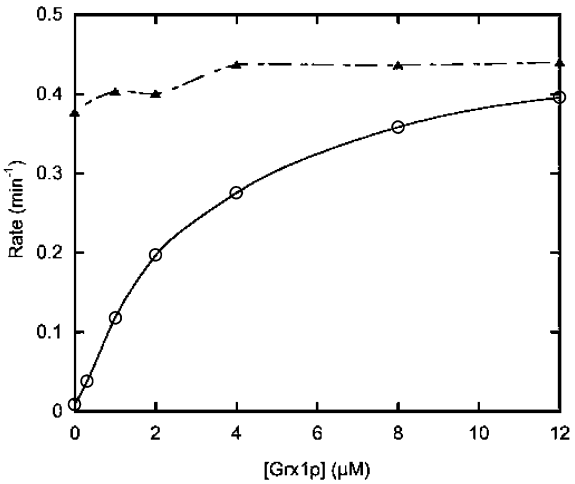

FIGURE 1: Grx dependence of the redox sensors during reduction by GSH. The redox sensors rxYFP (○) and rxYFP−Grx1p (▲) were reduced by GSH in the presence of varying concentrations of Grx1p. All reagents were diluted in standard buffer, and redox sensor and Grx1p were added in their oxidized forms. The redox sensor, in 1800 μL, was added to the fluorescence cuvette, followed by 100 μL of Grx1p, and the fluorescence signal was monitored during a preincubation for at least 5 min until a stable baseline was observed. The reduction was started by the addition of 100 μL of 400 mM GSH to a final concentration of 20 mM. Because of the content of GSSG (ca 0.3%) in the GSH stock solution, the final level of reduction was ca. 50%. The concentration of the redox sensor was 0.3 μM, and the reactions were followed to completion, except for the one in which no Grx1p was added to rxYFP. In this case, the rate was very low, and the reaction was followed for 90 min, to approximately half of its expected amplitude.

In the glutaredoxin assay, the fusion had approximately the same turnover number, 9 s^{-1}, as separate Grx1p, which is comparatively low among Grx's. Grx1 from *E. coli* has a 4-fold higher turnover number (*24*).

Reduction of the Fusion Protein by GSH. To determine whether Grx1p in the fusion to rxYFP acted in *cis* or *trans*, reduction of rxYFP and rxYFP−Grx1p by GSH was compared with respect to Grx1p dependence (Figure 1). In the absence of Grx1p, reduction and oxidation of rxYFP by GSH and GSSG are slow. In practice, overnight incubations are required to attain equilibrium, but the addition of catalytic amounts of Grx1p (<10 μM) enables equilibration within 10 min (*4*). Incubation of oxidized rxYFP in even fairly concentrated solutions of GSH (20 mM) from commercially available sources does not result in complete reduction. This is because of the difference in the standard redox potential between rxYFP (−265 mV) and GSH (−240 mV) and the fact that freshly prepared GSH solutions typically contain around 0.3% GSSG as determined by HPLC (data not shown). As seen in Figure 1, a very slow reduction of rxYFP was observed when Grx1p was omitted. The Grx1p-dependent increase in the rate showed an apparent saturation with respect to Grx1p toward a limiting rate of ca. 0.45 min^{-1}. In contrast, the reduction of rxYFP−Grx1p was largely independent of exogenous Grx1p, which caused only a moderate increase in the rate (<15%) over the same range of added Grx1p, and toward a similar limiting rate. The fusion protein can thus be described as essentially saturated with covalently linked Grx1p. Under the chosen conditions (0.3 μM rxYFP−Grx1p), the effective concentration of Grx1p as seen by the rxYFP partner can be estimated to ca. 10 μM. Furthermore, the rate of reduction with GSH was unaffected when the concentration of rxYFP−Grx1p was varied between 0.2 and 1.6 μM. On the basis of the observations above, we can conclude that catalysis is almost exclusively intramolecular.

Reduction by DTT and Standard Redox Potential of rxYFP−Grx1p. Because of its low standard redox potential [−308 mV (*27*)], DTT quantitatively reduces rxYFP and rxYFP−Grx1p. The apparent second-order rate constant for reduction of rxYFP−Grx1p was 19 M^{-1} min^{-1}, obtained from two independent experiments with four different concentrations of DTT in the range of 10−25 mM. This is a lower number than the 24.8 M^{-1} min^{-1} found for rxYFP (*2*). Thus, Grx1p, even when present as a fusion partner, does not catalyze DTT reduction of rxYFP−S_2; an expected observation if Grx1p is much less reducing than rxYFP. On the other hand, catalysis by Grx1p during GSH reduction, within the fusion or with isolated subunits (Figure 1), is consistent with a mechanism (Scheme 2) in which Grx1p−$(SH)_2$ attacks rxYFP−(SSG)(SH), i.e., the mixed disulfide between glutathione and rxYFP.

Reduced rxYFP was only oxidized very slowly (0.02 min^{-1}) by a 150-fold excess (50 μM) of Grx1p−S_2, but the reverse reaction, with a 150-fold excess of Grx1p$(SH)_2$, was at least 5 times slower. Because of the low rates of thiol−disulfide exchange and the practical difficulties of avoiding interference by atmospheric oxygen, these reactions only show that Grx1p is less reducing than rxYFP.

Åslund et al. (*28*) developed a method for determination of standard redox potentials (E_0 values) applicable to Grx and other thiol−disulfide oxidoreductases of the thioredoxin superfamily. By direct protein−protein redox equilibrium determinations with suitable standards (mutant forms of *E. coli* thioredoxin), the E_0 values of Grx1 and Grx3 from *E. coli* (both containing the active-site sequence CPYC) were determined to −230 and −200 mV, respectively. It is likely that the E_0' of Grx1p from yeast is in this range. We determined the stability of the 149−202 disulfide bond in the rxYFP−Grx1p fusion through its equilibrium with the GSH/GSSG couple by fluorescence as described for rxYFP (*4*). The equilibrium constant, K_{ox}, was 8.0 M (−267 mV), as compared to 6.8 M (−265 mV) for rxYFP. The attachment of an additional protein domain to rxYFP thus caused a slight but significant decrease in the standard redox potential of 2 mV.

Oxidation of the Fusion Protein by GSSG. The oxidation rate of rxYFP by GSSG was previously found to be 72 M^{-1} min^{-1} at pH 7 (*4*). Measurements with rxYFP−Grx1p were performed with up to 20 μM GSSG, and the apparent second-order rate constant was 2.4×10^5 M^{-1} min^{-1}, an enhancement of 3300-fold (Table 1), illustrating the dramatic effect of adding a functional Grx domain to rxYFP. The reaction showed simple monophasic kinetics below 5 μM GSSG, but above this concentration, the traces were biphasic (Figure 2A), with a second exponential rate constant of ca. 0.01 s^{-1} (0.6 min^{-1}) independent of the GSSG concentration (Figure 2B). The second component accounted for about 20% of the total amplitude.

We speculated that the biphasic reaction traces, observed only in oxidations with GSSG, were caused by two alternative pathways for the oxidation of the 149−202 dithiol in the rxYFP domain. In the first step toward oxidation, Grx

Scheme 2: Reduction and Oxidation of rxYFP by Grx1p and Glutathione

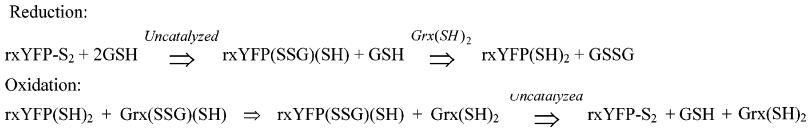

Table 1: Rates of Oxidation by GSSG, HED, Cystine, H_2O_2, and Cystamine[a]

	oxidant				
redox sensor	GSSG	HED	cystine	H_2O_2	cystamine
rxYFP	72[b]	35	1500	3.4	290
rxYFP−Grx1p	240 000	30[c]	1300[c]	3[c]	250
rxYFP−Grx1p-sC	1 800 000	220	21 000	180	290

[a] The reduced redox sensors were oxidized by at least four different concentrations, and the linear plots of the pseudo-first-order rate constant versus the concentration were used to obtain the apparent second-order rate constants (M^{-1} min^{-1}). [b] Value obtained from ref *4*. [c] The linear plot could be extrapolated to an intercept on the *y* axis of ca. 0.13 min^{-1}.

reacts with GSSG to form a mixed disulfide at the more N-terminal and exposed cysteine residue, Grx(SSG)(SH) (*7*). Through intramolecular attack from the remaining free cysteine, Grx(SSG)(SH) will eventually decompose into Grx disulfide, Grx−S_2, and one molecule of GSH. Both species, Grx(SSG)(SH) and Grx−S_2, might oxidize the 149−202 dithiol in the fusion, and to resolve whether this was the basis for the biphasic kinetics, we made a variant of the fusion sensor with the second cysteine of Grx mutated to serine. This variant, called rxYFP−Grx1p-sC, cannot form Grx−S_2. Interestingly, rxYFP−Grx1p-sC showed a further rate enhancement in the oxidation by GSSG by a factor of 7, to 1.8×10^6 M^{-1} min^{-1}. At GSSG concentrations above 3 μM, the reaction had a half-life (<10 s) similar to the time required for mixing. However, the biphasic character of the reaction traces was still present (data not shown). The second, GSSG-independent, rate component accounted for ca. 30% of the total amplitude and may be caused by a later step toward the formation of the 149−202 disulfide with quenched fluorescence.

Oxidation of rxYFP by Grx1p. To learn more about the interaction between rxYFP and Grx1p, we investigated the reaction between Grx1p and reduced rxYFP in their isolated forms. As mentioned above, the direct oxidation by GSSG is slow (72 M^{-1} min^{-1}), implying that the oxidation of rxYFP by 100 μM GSSG is hardly detectable within a time frame of a few minutes. In the experiment shown in Figure 3A, an excess of Grx1p$(SH)_2$ (5 μM) was first added to rxYFP-$(SH)_2$. When GSSG (100 μM) was added, a rapid oxidation of rxYFP followed. Thus, under these conditions, Grx1p is an active catalyst of rxYFP oxidation. In the next experiment (Figure 3B), Grx1p−S_2 (5 μM) was added to rxYFP$(SH)_2$. A stable baseline of the rxYFP emission was recorded for almost 10 min, which shows that Grx1p−S_2 is inefficient as an oxidant of rxYFP. When 100 μM of GSH was added to this mixture, a rapid oxidation of the redox sensor took place. These experiments show that, while GSSG and Grx1p−S_2 are inefficient as oxidants, the reactive species is the mixed disulfide with glutathione, Grx1p(SSG)(SH).

We wished to gauge the rate at which Grx1p(SSG)(SH) decomposed to Grx1p−S_2. Thus, the experiment shown in Figure 3A was repeated under conditions where Grx1p$(SH)_2$ had been preincubated with GSSG for 1 h at 30 °C to promote the formation of Grx1p−S_2, and the reaction was initiated by the addition of reduced rxYFP. However, the same oxidation rate (0.45 ± 0.02 min^{-1}) was obtained. Although the fraction of Grx1p present as Grx1p(SSG)(SH) is not inferred from these experiments, they demonstrate the oxidizing capacity and stability of the intermediate Grx1p-(SSG)(SH). They suggest that the rxYFP−Grx1p fusion almost exclusively uses Grx(SSG)(SH) for the oxidation of

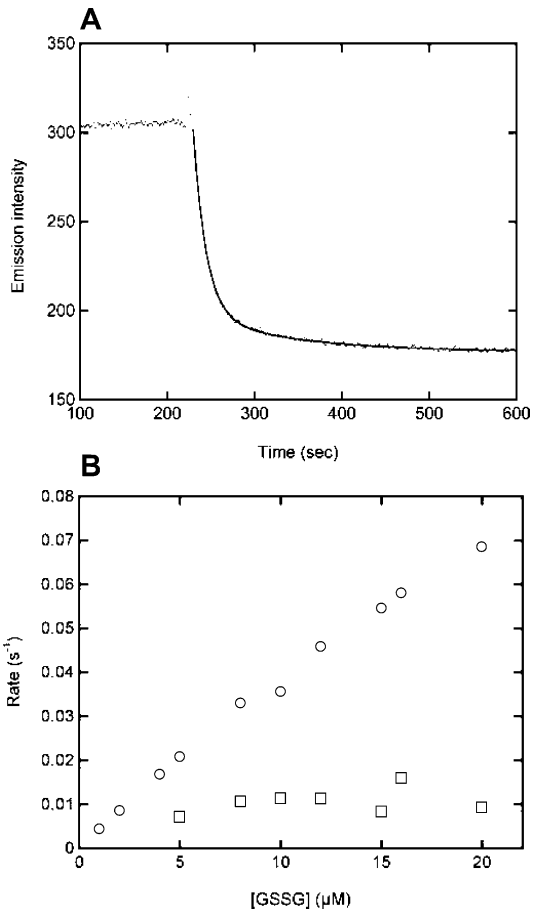

FIGURE 2: Oxidation of rxYFP−Grx1p with GSSG. (A) Oxidation of rxYFP−Grx1p by 20 μM GSSG. The addition of GSSG is seen as a small, transient rise in signal, and fitting of the subsequent reaction trace yielded the sum of two first-order reactions with the rate constants 0.0677 ± 0.0002 and 0.0093 ± 0.0001 s^{-1}, connected to two amplitudes for intensity changes of 103.0 ± 0.2 and 21.3 ± 0.2, respectively. The fluorescence cuvette contained reduced rxYFP−Grx1p (0.3 μM) in argon-saturated standard buffer, and after watching the baseline signal for 3−4 min, GSSG (1−20 μM) was added. (B) Two exponential rate components in the oxidation of rxYFP−Grx1p. The first component (○) showed a linear dependence on the GSSG concentration yielding an apparent second-order rate constant of 2.4×10^5 M^{-1} min^{-1}. The second component (□) accounted for ca. 20% of the change in signal and was independent of the GSSG concentration. All reaction traces were evaluated assuming biphasic reaction kinetics, but below 5 μM GSSG, the parameters obtained (amplitude and rate) for the second phase were negligible; i.e., simple monophasic kinetics were observed.

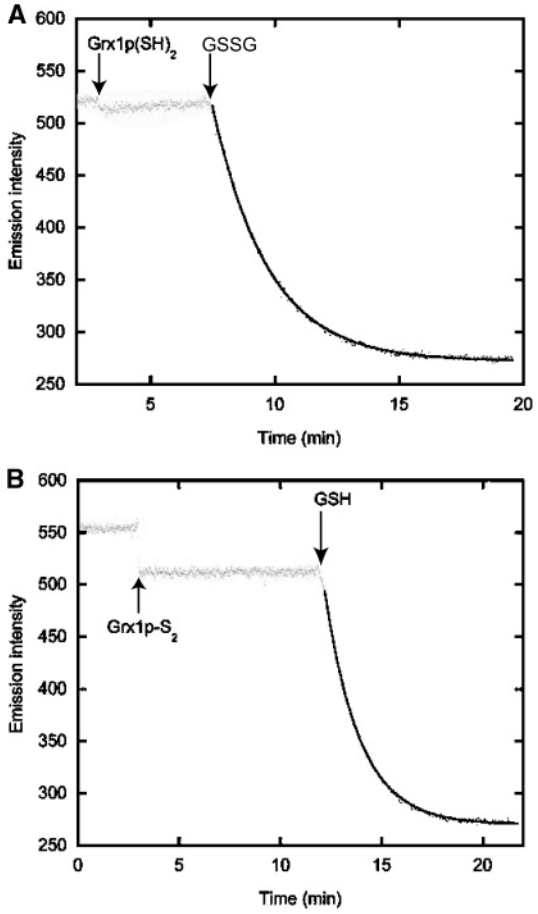

FIGURE 3: Oxidation of rxYFP by Grx1p. The oxidation of rxYFP-$(SH)_2$ by Grx1p and the influence of GSH and GSSG were monitored by fluorescence. At the start, the cuvette contained 0.3 μM of reduced rxYFP in 2 mL of standard buffer. (A) After 3 min, Grx1p$(SH)_2$ was added to 5 μM, followed by GSSG to 100 μM at 7 min. The addition of GSSG initiated the oxidation of $rxYFP_{red}$. (B) After 2.5 min, Grx1p$-S_2$ was added to 5 μM. The addition (100 μL of 106 μM Grx1p$-S_2$) is seen as a dilution of the fluorescence signal. After 12 min, GSH was added to 100 μM (2.1 μL of 100 mM GSH), resulting in fast oxidation.

the rxYFP domain, although it is capable of forming Grx$-S_2$. rxYFP$-$Grx1p-sC can only adopt one species for oxidation, rxYFP$-$Grx1p(SSG)(OH), which appears to be very efficient.

Reactions of the Fusion Proteins with Other Oxidants. The glutathione-binding site in conjunction with the redox-active cysteine residues are the hallmarks of Grx. Accordingly, the capability of rapid and glutathione-specific exchange reactions was conferred to the fusion proteins. Comparisons with the less specific oxidants, HED (Figure 4A), H_2O_2 (Figure 4B), cystine, and cystamine (Figure 4C), were also made. rxYFP, rxYFP$-$Grx1p, and rxYFP$-$Grx1p-sC were exposed to at least five different concentrations of each oxidant. HED is the standard substrate of the glutaredoxin assay (*24*). Only rather recently, H_2O_2 and organic peroxides were shown to be substrates of Grx's (*29*). rxYFP and rxYFP$-$Grx1p-sC displayed simple linear plots of pseudo-first-order kinetics versus the concentration of the oxidant, with lines passing through the $x-y$-axes intersection. The rate enhancement of rxYFP$-$Grx1p-sC compared to rxYFP was most pronounced, 50-fold, for H_2O_2 (Figure 4B and Table 1). For cystine and HED, the corresponding rate increases were 14- and 6-fold, respectively, while no rate increase was seen for cystamine.

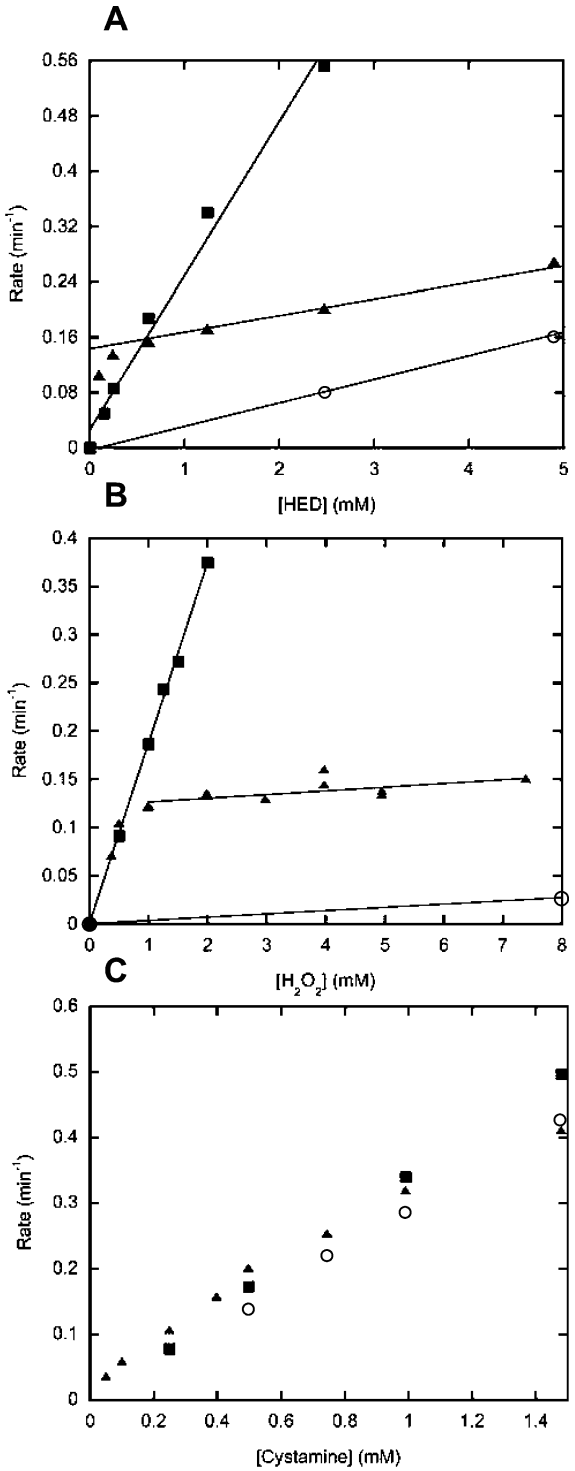

FIGURE 4: Oxidation of the redox sensors by HED, H_2O_2, and cystamine. The redox sensors, rxYFP (○), rxYFP$-$Grx1p (▲), and rxYFP$-$Grx1p-sC (■), were compared with respect to oxidation by HED (A), H_2O_2 (B), and cystamine (C). The oxidants were added to the reduced redox sensors, and the reactions were followed under standard conditions (30 °C, 0.1 M potassium phosphate and 1 mM EDTA at pH 7.0) and evaluated as described in the Experimental Procedures. For rxYFP, which showed comparatively low rates with H_2O_2 and HED, the linear plots are partly based on measurements at higher concentrations than those shown. Up to 30 and 10 mM were used for H_2O_2 and HED, respectively. Apparent second-order rate constants are presented in Table 1.

Surprisingly, the oxidation of rxYFP$-$Grx1p showed a dependence on the oxidant concentration, which was very different from those of rxYFP and rxYFP$-$Grx1p-sC. Low

concentrations of HED, H_2O_2, and cystine gave a rapid rise in the rate, but the further increases gave effects similar to those seen on rxYFP. For the three different oxidants, the further increases could be extrapolated back to a common intercept, of ca. 0.13 min^{-1}, on the *y* axis. The rate plot for cystamine did not show an intercept but was slightly skewed from linearity, and the rates for rxYFP and the two fusion proteins were all approximately similar (Figure 4C).

We interpret these results as follows: for oxidants different from glutathione, Grx1p−S_2 is rapidly formed via either the mixed disulfide (for HED or cystine) or the sulfenic acid formed by H_2O_2. The steep increase in the rate at low concentrations of oxidants represents a rate-limiting formation of Grx1p−S_2, and the break in the curve marks the effective saturation of Grx by the oxidant. Once Grx is saturated, direct oxidation of rxYFP by the oxidant becomes more and more dominant, giving rise to a linear increase, which is seen to be parallel for rxYFP and rxYFP−Grx1p. The intersection with the *y* axis represents the intramolecular transfer of a disulfide bond from Grx1p−S_2 to rxYFP, with a rate constant of 0.13 min^{-1}. The disulfide form of Grx accumulates because its subsequent reduction by rxYFP is slow (0.13 min^{-1}). For the oxidation of rxYFP−Grx1p-sC, the Grx−S_2 form cannot be made and the intermediate formed on the cysteine residue is subsequently free to oxidize rxYFP. Thus, the Grx−S_2 off-pathway is avoided, and the oxidation rate increases linearly over the whole concentration range. When rxYFP−Grx1p is oxidized by GSSG, the transfer of glutathione from Grx1p to rxYFP is much more rapid than the formation of Grx1p−S_2 and no *y*-axis intercept is seen (Figure 2B). The model also predicts that no clear intercept on the *y* axis will be seen if the rxYFP domain is oxidized to the disulfide form faster than the Grx domain. An example of this is seen with cystamine, which appears to react more rapidly with reduced rxYFP than with reduced Grx1p (Table 1 and Figure 4C). To assay the formation of Grx1p−S_2 directly, protection experiments were carried out on isolated Grx1p. When unreacted thiols are modified with PEG−maleimide, oxidation could be compared by SDS−PAGE. The poor reactivity of cystamine with Grx1p$(SH)_2$ relative to HED, H_2O_2, and cystine was confirmed, because it did not protect the enzyme from the reaction with PEG−maleimide (Figure 5).

A slow transfer of the disulfide bond to the rxYFP domain is relevant for the interpretation of the oxidation kinetics with GSSG, in which rxYFP−Grx1p-sC is 7 times faster than rxYFP−Grx1p. The formation of a disulfide bond in the Grx domain of rxYFP−Grx1p during the oxidation by GSSG would lead to the presence and accumulation of a slowly reacting species, but this is not observed (Figure 2B). Thus, both fusion sensors use the same mechanism, in which a glutathionylated intermediate on the reactive cysteine (C273) is transferred to rxYFP, and the slower oxidation of rxYFP−Grx1p by GSSG is not caused by the formation of an intramolecular disulfide in the Grx domain. Importantly, although Grx(SSG)(SH) does not readily release GSH, decomposition to Grx−S_2 of other mixed disulfides is fast, as seen, e.g., for rxYFP−Grx1p with HED (Figure 4A), which defines an efficient escape route for such mixed disulfides.

Alkylation of Grx1p and Grx1p-sC. To further examine the difference between native Grx with two cysteine residues

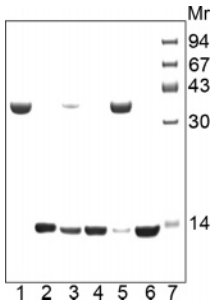

FIGURE 5: Protection of Grx1p$(SH)_2$ from modification by PEG−maleimide (5000 Da). Reduced and desalted Grx1p (65 μM) was incubated on ice with different oxidants at 0.5 mM. The incubations were terminated after 25 min by the addition of PEG−maleimide (5000 Da) to 0.6 mM and incubated on ice for 10 additional min. The modification was analyzed by reducing SDS−PAGE. (Lane 1) Grx1p$(SH)_2$ sample without added oxidant. (Lane 2) Neither oxidant nor PEG−maleimide was added. The reactions analyzed in the subsequent lanes were with H_2O_2 (lane 3), HED (lane 4), cystamine (lane 5), and cystine (lane 6), respectively. The increase in the mass is larger than 10 kDa for the dithiol Grx1p because PEG−maleimide binds water.

(CPYC) and the mutant form with only the more N-terminal one left (CPYS), we made the single-cysteine mutation, called Grx1p-sC, in the independent Grx1p domain. As seen for other members of the thioredoxin superfamily, structural studies of Grx's have shown that the first cysteine residue is exposed, while the second one is buried, consistently with earlier investigations using chemical modification (*30*−*32*). The effects of the CPYS mutation have been studied in many other Grx's. Both increases and decreases in glutaredoxin activity have been reported, certainly demonstrating that the second cysteine residue in the active site is not, like the first one, essential for the reaction. However, both cysteine residues are essential for the reduction of a protein disulfide like that in ribonucleotide reductase (*8*). In two cases, significant increases of activity have been reported for the CPYS mutation. Similar increases by a factor of 2 were reported for human Grx1 (thioltransferase) (*33*) and, recently, for human Grx2 (*34*). Grx1p-sC and the rxYFP−Grx1p-sC fusion displayed a 4-fold increase in activity in comparison to Grx1p and rxYFP−Grx1p. Yang et al. (*33*) explained the rise in activity of human Grx1 by the absence of a futile intramolecular reaction to Grx−S_2 (side reaction in Scheme 1) but also considered an alternative explanation, namely, an intrinsically higher reactivity of the remaining cysteine residue. Having seen the considerable stability of the intermediate Grx1p(SSG)(SH), we investigated the latter explanation.

The reactivity of a thiol is partly determined by its pK_a, and unusually low values, below 5.5, for the exposed cysteine residue in Grx have been concluded from alkylation studies of yeast Grx2p, *E. coli* Grx1, and pig liver Grx (*30*−*32*). Direct NMR observation of the thiol proton also supported an abnormally low pK_a in *E. coli* Grx3 (*35*). An interaction stabilizing the negative charge on the cysteine residue will tend to lower its pK_a value and, at the same time, decrease the nucleophilic character (*36*). To measure the reactivity of the exposed cysteine residue (C27) in native Grx1p in comparison to its reactivity in the single-cysteine context (CPYS), i.e., in the mutant Grx1p-sC, we followed the disappearance of activity during alkylation reactions at pH 7.0 (standard buffer). Although alkylation was very rapid

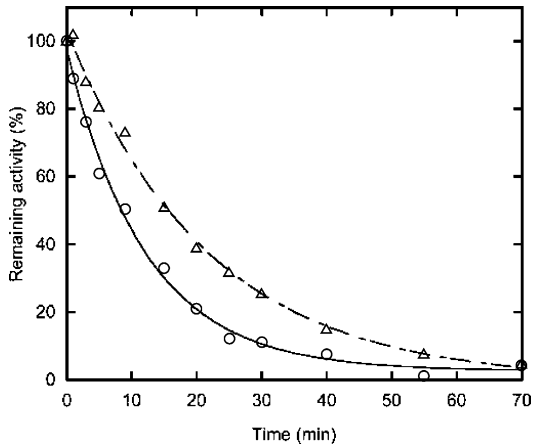

FIGURE 6: Alkylation of Grx1p and Grx1p-sC by iodoacetamide. Reduced and desalted enzyme (10 μM) in a volume of 700 μL was preincubated on ice in standard buffer for 30 min. The reaction was started by the addition of iodoacetamide to 200 μM, and aliquots of 40 μL were withdrawn at intervals. The aliquots were immediately diluted 10-fold in standard buffer containing 100 μM GSSG as a quenching agent and bovine serum albumin (0.1 mg/mL), and activity was measured the next day in the glutaredoxin assay (*24*). The presence of GSSG and iodoacetamide, up to 2.0 and 0.4 μM, respectively, did not disturb the assay. The result is presented as the remaining activity in comparison to an aliquot taken out before the addition of iodoacetamide (100%, corrected for dilution). For Grx1p (○) and Grx1p-sC (△), the first-order rate constants for the disappearance of activity were 0.082 ± 0.005 and 0.046 ± 0.003 min^{-1}, respectively.

even when carried out on an ice-water bath, the reactions were efficiently quenched by the oxidation of Grx with GSSG. Alkylation of Grx1p and Grx1p-sC by 200 μM iodoacetamide revealed a large difference in the rate (Figure 6). Grx1p was alkylated with a rate constant of 410 M^{-1} min^{-1}, while Grx1p-sC was alkylated 44% slower (230 M^{-1} min^{-1}). Only one of the cysteines, presumably the more N-terminal one (C27), reacted in Grx1p, because a control sample, alkylated for 1 h at a 15-fold higher concentration of iodoacetamide, still retained 0.87 equiv of thiol per enzyme molecule (as determined using Ellman's reagent). The slower alkylation of C27 in Grx1p-sC shows that it is less nucleophilic and indicates that, while it is not as efficient in attacking disulfides, it has a better leaving-group capability (i.e., a lower pK_a). The substitution of cysteine with serine involves no change of charge but may affect the strength of hydrogen bonds.

DISCUSSION

We have previously shown that rxYFP functions as a redox indicator of cytosolic glutathione in yeast cells because of the capacity of endogenous glutaredoxins to catalyze the equilibration between the sensor and the glutathione pool (*4*). This was found to be the case in yeast and could in principle be a peculiarity of Grx1p; therefore, it might not be generally true for other cells, e.g., of mammalian origin. Two rxYFP−Grx1p fusion proteins were made to extend the possible use to other organisms and improve the dynamic properties of rxYFP as a glutathione-specific redox sensor: a fusion with the native yeast Grx1p and a single-cysteine variant Grx1p-sC. We found that the two domains communicated intramolecularly, resulting in dramatically increased reaction rates. While the rate constant for oxidation by GSSG was increased by a factor of 25 000 for the rxYFP−Grx1p-sC fusion, specificity was superior for the rxYFP−Grx1p construct, which showed an almost 4000-fold increase in specificity toward GSSG relative to the biologically relevant disulfide cystine (Table 1). The results strongly suggest that the oxidation of rxYFP proceeds through the transfer of glutathione to generate a rxYFP(SSG)(SH) intermediate, which decomposes to rxYFP−S_2.

Experiments using isolated rxYFP and Grx1p showed that the disulfide form of Grx1p is inefficient as an oxidant of rxYFP (Figure 3). Within rxYFP−Grx1p, the disulfide form of the Grx domain (Grx−S_2) only reacts very slowly with the rxYFP dithiol. The transfer rate, 0.13 min^{-1}, can be compared to an example in nature. The large subunit of ribonucleotide reductase operates at a 1500-fold higher turnover number, and one of the required steps, which therefore has to be at least as fast, is the intramolecular transfer of a disulfide bond from one cysteine pair interacting with the ribonuceotide substrate to another pair interacting with the hydrogen-donor system (*37*). Apart from the redox equilibration of rxYFP, we are only aware of one example in which Grx has been shown to act as an oxidant *in vivo*. *E. coli* Grx1 catalyses disulfide bond formation in leaderless alkaline phosphatase in the oxidizing cytosol of combined null mutants of glutathione reductase and thioredoxin 1 (*38*). On the basis of the results with rxYFP, we suggest that the mixed disulfide with glutathione is employed in the formation of the disulfide bonds, consistently with a recent comparison of the *in vitro* oxidase activities of *E. coli* Grx1 and protein disulfide isomerase by Xiao et al. (*39*). Furthermore, the fusion proteins shed light on two connected but unresolved questions concerning the mechanism of Grx, namely, the kinetic stability of the mixed disulfide with glutathione and the consequences of a CPYS mutant. The reactivity of Grx1p with rxYFP provides information not available through steady-state kinetics.

Mutation of the second cysteine residue in the CPYC motif of Grx excludes Grx−S_2 offering the possibility to obtain stable mixed disulfides, and previous CPYS mutants have been rewarding for structural studies. There are three NMR structures with covalently bound glutathione in the active site, Grx(SSG)(OH), the first one of *E. coli* Grx1 (*40*). It was followed by the corresponding complex structures of human Grx1 (*33*) and *E. coli* Grx3 (*41*). In addition, the structure of the *E. coli* Grx1 CPYS mutant has been determined in covalent complex with a peptide mimicking the C terminus of the large subunit of ribonucleotide reductase (*42*). The binding of glutathione in an extended conformation in the three NMR structures of Grx(SSG)(OH) was roughly consistent with a previous model based on the X-ray structure of Grx from bacteriophage T4 (*43*).

While the structural studies have defined glutathione binding in three Grx's, our results demonstrate the kinetic stability of the intermediate Grx(SSG)(SH). The stability of the Grx(SSG)(SH) mixed disulfide is rather puzzling because one would expect the nearby second thiol to compete strongly for the disulfide. Only the NMR structure of *E. coli* Grx3-(SSG)(OH) offers a plausible explanation for stability of the intermediate Grx(SSG)(SH). On the basis of the assumption that the thiol group of the second cysteine residue would take up the same place as the hydroxyl group of the serine residue (in the monothiol mutant structure), the thiol group

is not in optimal position for intramolecular attack on the mixed disulfide (*41*). In addition, favorable interactions between the body of glutathione and glutaredoxin will serve to further stabilize the mixed disulfide. A comparison of the glutathione binding in the NMR structures of *E. coli* and human Grx1(SSG)(OH) revealed some differences with respect to the binding of the Gly carboxylate group of the glutathione moiety (*33*). Two residues involved in binding in human Grx1 (Q57 and R67) are conserved in Grx1p from yeast but not in *E. coli* Grx's. Therefore, Grx1p may be more related to human Grx1 than to *E. coli* Grx's, although the overall sequence identity is low in a pairwise comparison (ca 30%).

Separately or within the fusion, the Grx1p-sC mutant (CPYS) showed a 4-fold increase in oxidoreductase activity with HED as the substrate, while increases by a factor of 2 were reported for human Grx1 and Grx2 (*33*, *34*). The assay includes the classical substrate HED, and it implies pre-enzymatic formation of the preferred substrate, a mixed disulfide between HED and glutathione. To carry out the kinetic characterization of the human Grx1 CPYS mutant with "a true substrate", Yang et al. (*33*) used the mixed disulfide with cysteine (RSSG in Scheme 1) as a substrate together with GSH. With these two substrates, human Grx1 (and conceivably all Grx's) follows a simple Ping-Pong mechanism, in which the enzyme cycles, in two half reactions, between the fully reduced form, $Grx(SH)_2$, and the mixed disulfide, Grx(SSG)(SH), as shown by Gravina and Mieyal (*9*) (Scheme 1). It was found that the V_{max} and K_M for CSSG increased in parallel by a factor of 2 for the CPYS mutant, and it was proposed that the rise in activity was due to a rise in the concentration of the productive enzyme, because Grx(SSG)(SH) but not Grx(SSG)(OH) may transiently disappear from the half-reactions, by the formation of $Grx-S_2$ (side reaction in Scheme 1). Multiple stabilizing interactions are seen in the NMR structures of Grx(SSG)-(OH), and our results show that decomposition of Grx1p-(SSG)(SH) is extremely slow under standard conditions (pH 7.0). An alternative explanation for the increased reactivity is that the second half-reaction is running faster. In a Ping-Pong mechanism, it will indeed result in parallel increases of V_{max} and K_M of the substrate in the first half reaction. The reactivity of the exposed cysteine residue (C27) is markedly different in Grx1p and the Grx1p-sC mutant. The thiolate is less nucleophilic in the mutant, which has negative and positive effects on the first and second half reactions, respectively.

Despite a wealth of structural information on Grx's in general, the conformations of the active-site cysteine residues in the reduced form are difficult to define. Interestingly, a hydrogen bond between the thiol proton of the more C-terminal cysteine residue (C14) and the thiolate of the reactive cysteine residue (C11) in *E. coli* Grx3 was suggested (*35*). The thiol proton, having a remarkable chemical shift of 7.6 ppm, was proposed to donate a hydrogen bond to the thiolate. Subsequent modeling and a comparison to other proteins in the thioredoxin superfamily suggested this thiolate−thiol interaction as one of the key determinants behind the low pK_a of the thiolate (*44*). Our results suggest that a serine residue can act as an efficient hydrogen-bond donor, but at present, there is no structure available to substantiate or reject this speculation. The exchange of the more C-terminal cysteine residue into serine in Grx is not only a conservative substitution; improved leaving-group capability makes the enzyme better as a donor of a glutathione moiety, which may be pertinent to the role of native monothiol Grx's.

ACKNOWLEDGMENT

We thank Kresten Lindorff-Larsen and Morten Kielland-Brandt for useful discussions and critical reading of the manuscript.

REFERENCES

1. Tsien, R. Y. (1998) The green fluorescent protein, *Annu. Rev. Biochem. 67*, 509−544.
2. Ostergaard, H., Henriksen, A., Hansen, F. G., and Winther, J. R. (2001) Shedding light on disulfide bond formation: Engineering a redox switch in green fluorescent protein, *EMBO J. 20*, 5853−5862.
3. Hanson, G. T., Aggeler, R., Oglesbee, D., Cannon, M., Capaldi, R. A., Tsien, R. Y., and Remington, S. J. (2004) Investigating mitochondrial redox potential with redox-sensitive green fluorescent protein indicators, *J. Biol. Chem. 279*, 13044−13053.
4. Ostergaard, H., Tachibana, C., and Winther, J. R. (2004) Monitoring disulfide bond formation in the eukaryotic cytosol, *J. Cell Biol. 166*, 337−345.
5. Dooley, C. T., Dore, T. M., Hanson, G. T., Jackson, W. C., Remington, S. J., and Tsien, R. Y. (2004) Imaging dynamic redox changes in mammalian cells with green fluorescent protein indicators, *J. Biol. Chem. 279*, 22284−22293.
6. Holmgren, A. (1989) Thioredoxins and glutaredoxin systems, *J. Biol. Chem. 264*, 13963−13966.
7. Fernandes, A. P., and Holmgren, A. (2004) Glutaredoxins: Glutathione-dependent redox enzymes with functions far beyond a simple thioredoxin system, *Antioxid. Redox Signaling 6*, 63−74.
8. Bushweller, J. H., Åslund, F., Wuthrich, K., and Holmgren, A. (1992) Structural and functional characterization of the mutant *Escherichia coli* glutaredoxin(C14-S) and its mixed disulfide with glutathione, *Biochemistry 31*, 9288−9293.
9. Gravina, S. A., and Mieyal, J. J. (1993) Thioltransferase is a specific mixed disulfide oxidoreducatse, *Biochemistry 32*, 3368−3376.
10. Fernandes, A. P., Fladvad, M., Berndt, C., Andresen, C., Lillig, C. H., Neubauer, P., Sunnerhagen, M., Holmgren, A., and Vlamis-Gardikas, A. (2005) A novel monothiol glutaredoxin (Grx4) from *Escherichia coli* can serve as a substrate for thioredoxin reductase, *J. Biol. Chem. 280*, 24544−24552.
11. Fladvad, M., Bellanda, M., Fernandes, A. P., Mammi, S., Vlamis-Gardikas, A., Holmgren, A., and Sunnerhagen, M. (2005) Molecular mapping of functionalities in the solution structure of reduced Grx4, a monothiol glutaredoxin from *Escherichia coli*, *J. Biol. Chem. 280*, 24553−24561.
12. Luikenhuis, S., Perrone, G., Dawes, I. W., and Grant, C. M. (1998) The yeast *Saccharomyces cerevisiae* contains two glutaredoxin genes that are required for protection against reactive oxygen species, *Mol. Biol. Cell 9*, 1081−1091.
13. Molina, M. M., Belli, G., de la Torre, M. A., Rodrigues-Manzaneque, M. T., and Herrero, E. (2004) Nuclear monothiol glutaredoxins of *Saccharomyces cerevisiae* can function as mitochondrial glutaredoxins, *J. Biol. Chem. 279*, 51923−51930.
14. Lundberg, M., Johansson, C., Chandra, J., Enoksson, M., Jacobsson, G., Ljung, J., Johansson, M., and Holmgren, A. (2001) Cloning and expression of a novel human glutaredoxin (Grx2) with mitochondrial and nuclear isoforms, *J. Biol. Chem. 276*, 26269−26275.
15. Gladyshev, V. N., Liu, A., Novoselov, S. V., Krysan, K., Sun, Q.-A., Kryukov, V. M., Kryukov, G. V., and Lou, M. F. (2001) Identification and characterization of a new mammalian glutaredoxin (thioltransferase), Grx2, *J. Biol. Chem. 276*, 30374−30380.
16. Lundberg, M., Fernandes, A. P., Kumar, S., and Holmgren, A. (2004) Cellular and plasma levels of human glutaredoxin 1 and 2 detected by sensitive ELISA systems, *Biochem. Biophys. Res. Commun. 319*, 801−809.
17. Song, J. J., Rhee, J. G., Suntharalingam, M., Walsh, S. A., Spitz, D. R., and Lee, Y. J. (2002) Role of glutaredoxin in metabolic oxidative stress, *J. Biol. Chem. 277*, 46566−46575.

18. Starke, D. W., Chock, P. B., and Mieyal, J. J. (2003) Glutathione−thiyl radical scavenging and transferase properties of human glutaredoxin (thioltransferase). Potential role in redox signal transduction, *J. Biol. Chem. 278*, 14607−14613.
19. Ho, S. N., Hunt, H. D., Horton, R. M., Pullen, J. K., and Pease, L. R. (1989) Site-directed mutagenesis by overlap extension using the polymerase chain reaction, *Gene 77*, 51−59.
20. Topell, S., Hennecke, J., and Glockshuber, R. (1999) Circularly permutated variants of the green fluorescent protein, *FEBS Lett. 457*, 283−289.
21. Gill, S. C., and Hippel, P. H. (1989) Calculation of protein extinction coefficients from amino acid sequence data, *Anal. Biochem. 182*, 319−326.
22. Ellman, G. L. (1959) Tissue sulfhydryl groups, *Arch. Biochem. Biophys. 82*, 70−77.
23. Chau, M. H., and Nelson, J. W. (1991) Direct measurement of the equilibrium between glutathione and dithiothreitol by high performance liquid chromatography, *FEBS Lett. 291*, 296−298.
24. Holmgren, A., and Åslund, F. (1995) Glutaredoxin, *Methods Enzymol. 252*, 283−292.
25. Rost, J., and Rapoport, S. (1964) Reduction-potential of glutathione, *Nature 201*, 185.
26. Li, X., Zhang, G., Ngo, N., Zhao, X., Kain, S. R., and Huang, C.-C. (1997) Deletions of the *Aequorea victoria* green fluorescent protein define the minimal domain required for fluorescence, *J. Biol. Chem. 272*, 28545−28549.
27. Rothwarf, D. M., and Scheraga, H. A. (1992) Equilibrium and kinetic constants for the thiol−disulfide interchange reaction between glutathione and dithiothreitol, *Proc. Natl. Acad. Sci. U.S.A. 89*, 7944−7948.
28. Åslund, F., Berndt, K. D., and Holmgren, A. (1997) Redox potentials of glutaredoxins and other thiol−disulfide oxidoreductases of the thioredoxin superfamily detemined by direct protein−protein redox equilibria, *J. Biol. Chem. 272*, 30780−30786.
29. Collinson, E. J., Wheeler, G. L., Garrido, E. O., Avery, A. M., Avery, S. V., and Grant, C. M. (2002) The yeast glutaredoxins are active as glutathione peroxidases, *J. Biol. Chem. 277*, 16712−16717.
30. Gan, Z.-R., Sardana, M. K., Jacobs, J. W., and Polokoff, M. A. (1990) Yeast thioltransferase−The active site cysteines display differential reactivity, *Arch. Biochem. Biophys. 282*, 110−115.
31. Björnberg, O. (1990) Master Thesis, Karolinska Institutet, Stockholm, Sweden.
32. Yang, Y., and Wells, W. W. (1991) Identification and characterization of the functional amino acids at the active center of pig liver thioltransferase by site-directed mutagenesis, *J. Biol. Chem. 266*, 12759−12765.
33. Yang, Y., Jao, S., Nanduri, S., Starke, D. W., Mieyal, J. J., and Qin, J. (1998) Reactivity of the human thioltransferase (glutaredoxin) C7S, C25S, C78S, C82S mutant and NMR solution structure of its glutathionyl mixed disulfide intermediate reflect catalytic specificity, *Biochemistry 37*, 17145−17156.
34. Johansson, C., Lillig, C. H., and Holmgren, A. (2004) Human mitochondrial glutaredoxin reduces *s*-glutathionylated proteins with high affinity accepting electrons from either glutathione or thioredoxin reductase, *J. Biol. Chem. 279*, 7537−7543.
35. Nordstrand, K., Åslund, F., Meunier, S., Holmgren, A., Otting, G., and Berndt, K. D. (1999) Direct NMR observation of the Cys-14 thiol proton of reduced *Escherichia coli* glutaredoxin-3 supports the presence of an active site thiol−thiolate hydrogen bond, *FEBS Lett. 449*, 196−200.
36. Szajewski, R. P., and Whitesides, G. M. (1980) Rate constants and equilibrium constants for thiol−disulfide interchange reactions involving glutathione, *J. Am. Chem. Soc 102*, 2011−2025.
37. Stubbe, J. (1990) Ribonucleotide reductases: Amazing and still confusing, *J. Biol. Chem. 265*, 5329−5332.
38. Vlamis-Gardikas, A., Potamitou, A., Zarivach, R., Hochman, A., and Holmgren, A. (2002) Characterization of *Escherichia coli* null mutants for glutaredoxin 2, *J. Biol. Chem. 277*, 10861−10868.
39. Xiao, R., Lundström-Ljung, J., Holmgren, A., and Gilbert, H. F. (2005) Catalysis of thiol/disulfide exchange: Glutaredoxin 1 and protein disulfide isomerase use different mechanisms to enhance oxidase and reductase activities, *J. Biol. Chem. 280*, 21099−21106.
40. Bushweller, J. H., Billeter, M., Holmgren, A., and Wuthrich, K. (1994) The nuclear magnetic resonance solution structure of the mixed disulfide between *Escherichia coli* glutaredoxin(C14S) and glutathione, *J. Mol. Biol. 235*, 1585−1597.
41. Nordstrand, K., Åslund, F., Holmgren, A., Otting, G., and Berndt, K. D. (1999) NMR structure of *Escherichia coli* glutaredoxin 3-glutathione mixed disulfide complex: Implications for the enzymatic mechanism, *J. Mol. Biol. 286*, 541−552.
42. Berardi, M. J., and Bushweller, J. H. (1999) Binding specificity and mechanistic insight into glutaredoxin-catalyzed protein disulfide reduction, *J. Mol. Biol 292*, 151−161.
43. Nikkola, M., Gleason, F. K., Saarinen, M., Joelson, T., Björnberg, O., and Eklund, H. (1991) A putative glutathione-binding site in T4 glutaredoxin investigated by site-directed mutagenesis, *J. Biol. Chem. 266*, 16105−16112.
44. Foloppe, N., Sagemark, J., Nordstrand, K., Berndt, K. D., and Nilsson, L. (2001) Structure, dynamics, and electrostatics of the active site of Glutaredoxin 3 from *Escherichia coli*: Comparison with functionally related proteins, *J. Mol. Biol. 310*, 449−470.

BI0522495